

Modelling the cracking of fresh concrete

Riaan Combrinck^{1,*}, Marnu Meyer¹ and William P. Boshoff²

¹Stellenbosch University, South Africa

²University of Pretoria, South Africa

Abstract. The cracking of fresh concrete, while still in a plastic state, includes both plastic settlement and plastic shrinkage cracking, which starts once the concrete is cast to around the final setting time. The cracking process is complex and is influenced by numerous factors which include the climate, mix proportions, element geometry and construction procedures. Preventing these cracks therefore remains a problem in practice. One of the reasons for this is the lack of a model that can be used to determine the location, timing and severity of the cracking before the cracking occurs. The main challenges with such a model are the testing of the fresh concrete to determine the tensile material properties, the appropriate constitutive law needed, and the time dependency of material properties as well as the anisotropic volume change. This paper presents a finite element model that uses a total strain smeared cracking approach and accounts for both the time dependency of material properties and the anisotropic volume change. The model gives an adequate representation of the cracking behaviour of fresh concrete for extreme climates but not for normal to moderate climates, mainly due to the size discrepancy between the interior and surface cracks during experiments as well as the relaxation of stresses that are not accounted for in the model. A parameter study showed that both the settlement and shrinkage strains significantly influence and therefore govern the size of the final plastic crack, while the material mechanical properties only influence the time of crack onset and rate of crack widening.

1. Introduction

The cracking of fresh concrete is a complex process with various influencing factors such as environmental conditions, mix proportions, construction procedures, concrete element geometry, restraint and time. For conventional concrete there are two types of plastic cracking, called plastic settlement and plastic shrinkage cracking. Plastic settlement cracking is caused by differential settlement within the concrete body [1-3] while plastic shrinkage cracking is caused by the evaporation of water within the concrete pore system [4, 5]. Both cracking types can occur separately as well as combined, further increasing the complexity [2, 3].

Preventing these cracks remains a problem in practice. One of the reasons for this is the lack of knowledge of when, where and how severe the cracking is going to be before the structure is build. The general guidance given up to date is that these cracks are likely to occur if the evaporation rate is more than 1 kg/m²/h [6, 7] and if so the appropriate preventative measures, mostly aimed at minimising the evaporation, should be taken. This creates a need for a model that can be used to determine the location, timing and size of the cracking before the cracking occurs.

The modelling of cracking in fresh concrete can and has been approached on three different levels namely the micro-, meso- and macro level. Micro level modelling considers all the constituents of the concrete such as the different solid particles and water individually as well as

the physical and chemical processes influencing those [8, 9].

Meso level modelling differentiates between the cement paste and the aggregates as well as the physical processes that influence these phases [10].

Macro level modelling homogenizes the behaviour of the structure by considering the entire structure or body as a whole. These models use average values for important material parameters which smear out any differences that might be present in the internal structure of the concrete [8]. The model also consider external conditions such as loads and boundary conditions. All the constitutive laws that describe the behaviour of the structure are combined into governing equations (usually differential equations) which are solved for the entire structure normally by using finite element methods.

For this paper a macro level finite element approach based on continuum mechanics is used to model the cracking behaviour of fresh concrete. This approach requires information such as boundary conditions, material properties, loading and constitutive laws that govern material behaviour. Literature regarding the finite element modelling of cracking in fresh concrete is rare and this is partly due to the complexity involved with the cracking of fresh concrete.

One of the biggest challenges is the significant and relatively rapid change of the concrete from a plastic material to a weak-solid within a couple of hours. This means that the behaviour of the concrete also changes

* Corresponding author : rcom@sun.ac.za

from a ductile to a quasi-brittle material, while the material properties such as strength, stiffness and fracture energy also change dramatically with time as the concrete sets and strengthens. These material parameters are typically needed as input values for a model. For hardened concrete these parameters are normally determined by direct or indirect tensile tests on concrete samples. However, these type of tests present a much bigger challenge if conducted on fresh concrete samples [11], and requires a test setup capable of performing the challenging tensile tests on a still fresh concrete.

Furthermore, the volume change associated with fresh concrete is also time dependent and includes settlement which starts once the concrete has been cast as well as plastic shrinkage which starts once concrete pore water is removed by evaporation. In addition, the settlement and shrinkage do not start or end at the same time, while the rate and magnitude of both also change with time. The complexity is further increased by the anisotropic nature of the settlement and shrinkage, where settlement is a one dimensional volume change and plastic shrinkage is a volumetric volume change [3, 5]. The model needs to account for the time dependency of material properties and volume change as well as the anisotropic nature of the volume change.

Another challenge is the constitutive law that governs the behaviour of the material under loading. The constitutive model applicable to the cracking behaviour of fresh concrete is not well researched or defined in literature. Some of the available models in literature, as discussed in the introduction, simulated the cracking by searching for equilibrium of numerous forces acting on individual solid particles in a cement paste [9], while others used theories such as the consolidation of soils to model the settlement of concrete [2].

Although there are some challenges faced with developing a model, it is an important step towards ultimately completely preventing these cracks in concrete structures. This paper proposes and discusses the results achieved with a finite element model that accounts for all the mentioned challenges.

2. Experimental setup and results

Input data for the finite element model, such as the free shrinkage and settlement strains, tensile strength, Young's modulus and fracture energy, needs to be determined with experiments. For the purpose of this paper a brief description of the test setup and results achieved follows. A more in depth discussion of the test setup and test results can be found elsewhere [12]. A conventional concrete mix with water cement (w/c) ratio of 0.6, slump of 70 mm and 28 day cube compression strength of 38 MPa was used for all tests. In addition, all tests were conducted at a moderate and extreme environmental condition which has evaporation rates of approximately 0.5 and 1 kg/m²/h, respectively, based on Uno's [6] equation. At least 3 test samples were used for all tests conducted and an average reported. Table 1 and Table 2 provide details regarding the material constituents of the concrete mix and environmental conditions used, respectively.

Table 1. Material constituents of concrete mix in kg/m³.

Water	205
Cement - CEM II 52.5N	342
13 mm Greywacke stone	1037
Natural quarry sand	569
Greywacke crusher dust - sieved through 2.36 mm sieve	244

Table 2. Environmental conditions.

Climatic condition	Moderate	Extreme
Concrete temperature [°C]	23	23
Ambient temperature [°C]	23	40
Relative humidity [%]	60	10
Wind speed [km/h]	21	21

The tensile material properties of the fresh concrete was determined using a direct tensile test setup. The setup consists of a support structure, air bearing, mechanical linear actuator and dog bone shape mould as shown in Fig. 1. The air bearing floats the mould using an ultra-thin film of air, while the actuator applies the horizontal load. The load is measured using a 2 kN HBM load cell at the stationary end of the setup, while the displacements are measured on the concrete over the gauge length using a linear variable displacement transducer (LVDT).

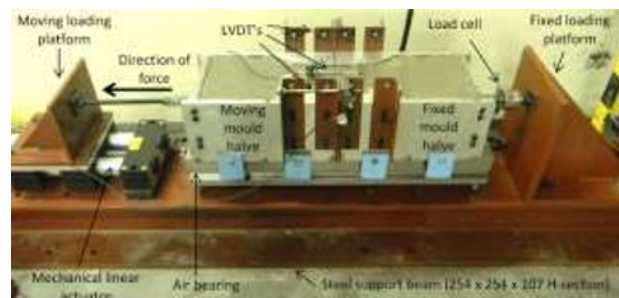


Fig. 1. Direct tensile test setup.

Tests were performed at hourly intervals up to a maximum of 6 hours, where a new sample was used for every test. The measurements were used to determine stress-strain graphs, from which the needed tensile material parameters could be determined as illustrated in Fig. 2.

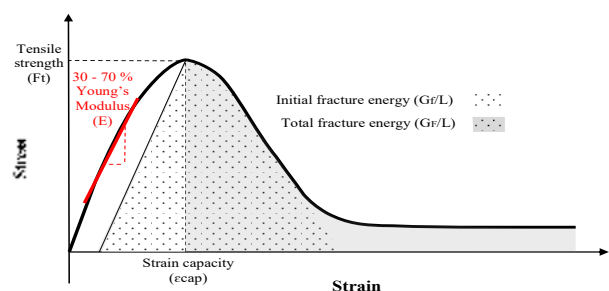


Fig. 2. Illustration of typical stress-strain curve.

Fig. 2 shows that the Young's modulus was determined as the gradient of a linear trend line that was fitted the ascending portion of the graph between 30 and 70% of the tensile strength. This approach differs from tradition approaches [13, 14] and was chosen to obtain a better representative Young's modulus that is not dominated by either the initial elastic part or final plastic part of the curve. This also better accounts for the significant differences between the stress strain graphs from testing at an age of 1 to 6 hour tests as the concrete changes from a plastic and ductile material to solid and quasi-brittle material. In addition, the initial fracture energy is used and not the total fracture energy as shown in Fig. 2. The reason for this is the difficulty in capturing the post peak softening curve during testing without the influence of friction due to skewing.

The average results achieved in terms of tensile strength, Young's modulus and initial fracture energy at both the moderate and extreme climates are shown in Fig. 3 to Fig. 5. It should be noted that the surface of the test samples were closed using damp blankets to avoid capillary pressure build up due to evaporation and thereby avoid any residual stresses in the concrete before testing. This means these samples were only exposed to the 23 and 40°C air temperature and not the wind and relative humidity of the moderate and extreme climates.

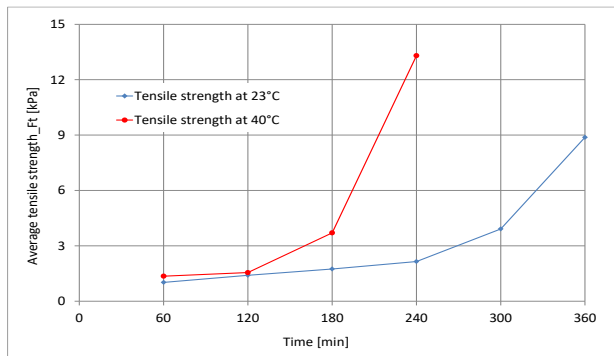


Fig. 3. Average tensile strength (F_t) development with time at 23 and 40°C.

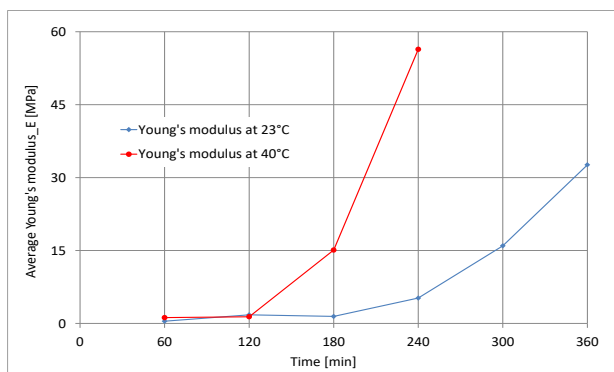


Fig. 4. Average Young's modulus (E) development with time at 23 and 40°C.

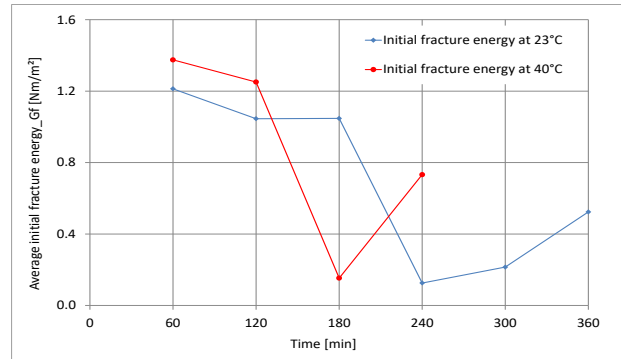


Fig. 5. Average initial fracture energy (G_f) development with time at 23 and 40°C.

Finally, as verification of the model results, the actual cracking that occurs within a mould is required. Moulds based on the ASTM C1579 [15] mould were used and modified to increase restraint by adding an additional steel bar at each end [16]. The free settlement and shrinkage was determined using the setup proposed by Slowik et al. [5]. Fig. 6 shows the results for free shrinkage and settlement strains as well as the average crack widths as measured for both climates. The cracks were measured using high resolution surface images and digital imaging processing. More information on these test and the measurement techniques can be found elsewhere [17]

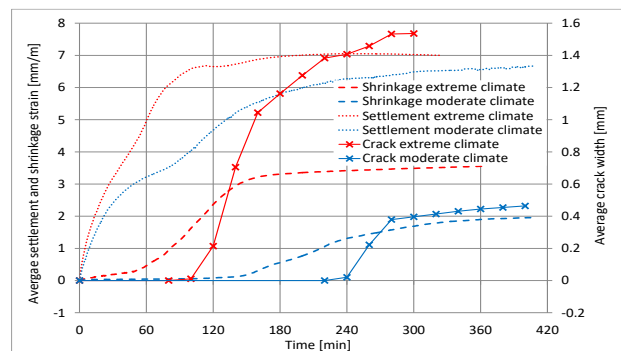


Fig. 6. Average free shrinkage and settlement strain as well as average crack width as measured in ASTM C1579 based mould at both the moderate and extreme climate.

3. Model framework

This section describes the proposed finite element model for simulating the cracking behaviour of fresh concrete. The software package DIANA Version 9.6 [18] was used for the modelling.

3.1. Constitutive material law

This paper adopted one of the several existing constitutive crack models that are already well establish and used for mature concrete. The smeared rotating crack model that uses fracture energy and a crack band width for crack propagation was chosen.

Continuous cracking, also referred to as smeared cracking, was chosen since the crack location was not known beforehand [19]. The rotating crack model was chosen to ensure the crack orientation remains perpendicular to the principal strain direction, which ensures that no shear stress develops over the crack plane,

removing the possibility of a normal stress exceeding the tensile stress in another direction [20]. A tension softening stress-strain relationship that is based on fracture energy to govern crack propagation and related to a crack band width was chosen to prevent mesh dependent release of energy [21].

The rotating total strain cracking model available in the DIANA [18] was chosen to achieve this. This model uses a coaxial stress-strain concept where the stress-strain relationship is the same in both tension and compression in the elastic region, together with a smeared cracking approach for the tension softening part of the stress-strain curve using fracture energy and a crack band width.

The total strain concept further assumes an injective (one to one) relationship between stress and strain, where the total strain field is taken as a combination of the concrete strain and the cracking strain [21]. This allows the constitutive behaviour of the concrete to be modelled separately from the cracking behaviour at the crack location. This means the strain due to crack opening is added to the total strains at a material point. Total strain models have been shown to work for various applications and are especially suited for serviceability and ultimate limit state analyses that are dominated by the cracking of concrete in the tensile regime [18]. The drawback of total strain models is that they cannot be combined with other constitutive models within the same material, although they can be combined with ambient influences [18].

3.2. Geometry, elements and boundary conditions

Fig. 7 shows the finite element mesh as well as boundary conditions that are used to model the experiments. The mesh size is consistent, with the dimensions of all the elements at 5 x 5 mm. The model further uses linearly interpolated four node quadrilateral isoparametric plane stress elements. The thickness of the elements are 200 mm which corresponds to the width of the mould.

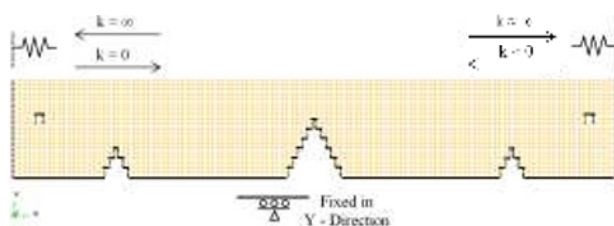


Fig. 7. Finite element mesh including the boundary conditions used to model the cracking in the ASTM C1579 [15] based mould.

All the elements in contact with the bottom of the mould or other fixed horizontal surfaces (restraining inserts) are fixed in the y-direction but free to move in the x-direction. The vertical boundary conditions at the ends of the mould and other fixed vertical surfaces are more complex as these boundary conditions should allow movement of the elements away from the fixed surface but not towards it. To achieve this, one-node axial translational spring elements are placed at all nodes that exists between the vertical surfaces of the mould and the four node plane stress elements.

The spring elements were placed at the left and right vertical boundaries surfaces. These springs allow the fresh concrete to move away from the vertical mould surfaces due to settlement and shrinkage, but also support and prevent movement in the opposite direction past or into mould vertical surfaces. These boundary conditions therefore assume that there is no adhesion or friction between the mould and the concrete.

3.3. Material parameters

The parameters needed for a total strain crack model are the tensile strength (F_t), Young's modulus (E) and fracture energy (G_f), all as a function of time. A linear tension softening curve [18] based on fracture energy which is smeared over a crack band width (h) is chosen as this best represents the initial fracture energy (G_f) values obtained during the experiments.

The crack band width was chosen as a constant value of 5 mm, which is the width of the four node plane stress elements used. This is acceptable for the release of the correct amount of fracture energy after cracking as long as the crack remains perfectly vertical or horizontal and does not skew. For skew cracks, it is better to use a crack band width equal to the square root of twice the area of the element [18]. Finally, the Poisson's ratio is chosen as zero, since it is believed that its influence is insignificant, since the measured vertical settlement and horizontal shrinkage strains as used in the model include the possible effect of Poisson's ratio.

The experimental material properties were tested at hourly intervals while the model was analysed at smaller time steps of 20 minutes. The material properties at these smaller time intervals were linearly interpolated. It was also assumed that the values of the material properties at 0 hours are the same as determined at 1 hour.

3.4. Loading

The settlement and shrinkage of fresh concrete act as applied loads on the concrete as for a traditional model. The volume change of fresh concrete is anisotropic, meaning different magnitudes and rates of strain in both the vertical and horizontal directions.

The plastic shrinkage is modelled as a function of time using the discrete shrinkage function available in DIANA [18]. This shrinkage strain as specified at each specific time is added to the concrete strain which allows this discrete shrinkage function to be used in conjunction with the total strain crack model [21]. This function also assumes isotropic shrinkage, meaning that shrinkage strains are the same in both the vertical and horizontal directions. However, the measured shrinkage in the experiments, as shown in Fig. 6, is only in the horizontal direction and hence the vertical shrinkage imposed by the discrete shrinkage function in the model is incorrect.

This is accounted for by using a method that models the plastic settlement by gradually increasing the own weight of the elements with time to such an extent as to result in a deformation due to own weight that is equal to the experimentally measured vertical settlement. This is achieved by changing the load factor applied to the gravitational acceleration used to calculate the own weight of the elements for each time interval. To account

for the incorrect vertical plastic shrinkage applied by the discrete shrinkage function, the load factor responsible for the settlement due to own weight is calculated using the measured settlement strains minus the vertical shrinkage strains imposed by the discrete shrinkage function. This allows the appropriate measured shrinkage and settlement strains to be directly specified for each time step used in the model.

3.5. Analysis description

The model is executed using a physical non-linear time dependent analysis that employs an incremental-iterative procedure in a series of time steps. The regular Newton-Raphson iteration procedure is used together with a tangent stiffness matrix, since this approach proved to be robust and stable for analyses with crack localisation and propagation [18]. Furthermore, an energy convergence criterion is used where convergence is reached in an iteration of a specific time step once the resultant energy variation relative to an equilibrium state is less than 0.00001. The time steps are increased in 20 minute increments for all analyses.

4. Modelling results

The results achieved with the model should be compared against the actual measured crack widths as shown in Fig. 6. In the following sections the modelling results are evaluated and compared with the measured cracks in terms of the final crack size, time of crack onset as well as the rate at which the cracking occurs for both the extreme and moderate climate. This is followed by a parameter study.

4.1. Model validation at extreme climate

The model results at the extreme climate where all the elements are given cracking behaviour are shown in Fig. 8. The figure shows the resultant displacements of the mesh in undeformed and deformed shape as well as the maximum principle tensile strain in the elements at progressive time steps in the analysis. The localisation of strain indicates cracks, with the most notable and severe crack located above the central triangular restraint. Smaller cracks also occurred from the tip of the smaller triangular restraints upwards as well as around the steel bar at both ends of the mould. This included two shear cracks starting from the sides of the steel bar as well as a tensile crack at the surface above the steel bar, similar to the plastic settlement cracks observed by Combrinck et al. [3].

Similar cracks were also observed during the experiments as shown in Fig. 9. The figure shows the typical final cracks that were visible from the side of the mould with the Perspex side cover removed. The figure clearly shows the major crack above the central triangular restraint as well as the smaller cracks around the steel bars and smaller triangular restraints. Furthermore, the model result in Fig. 8 shows additional cracking next to the central triangular restraint which was not visible during experiments as shown in Fig. 9. These cracks next to the central triangular restraint became more severe as time progressed in the analysis.

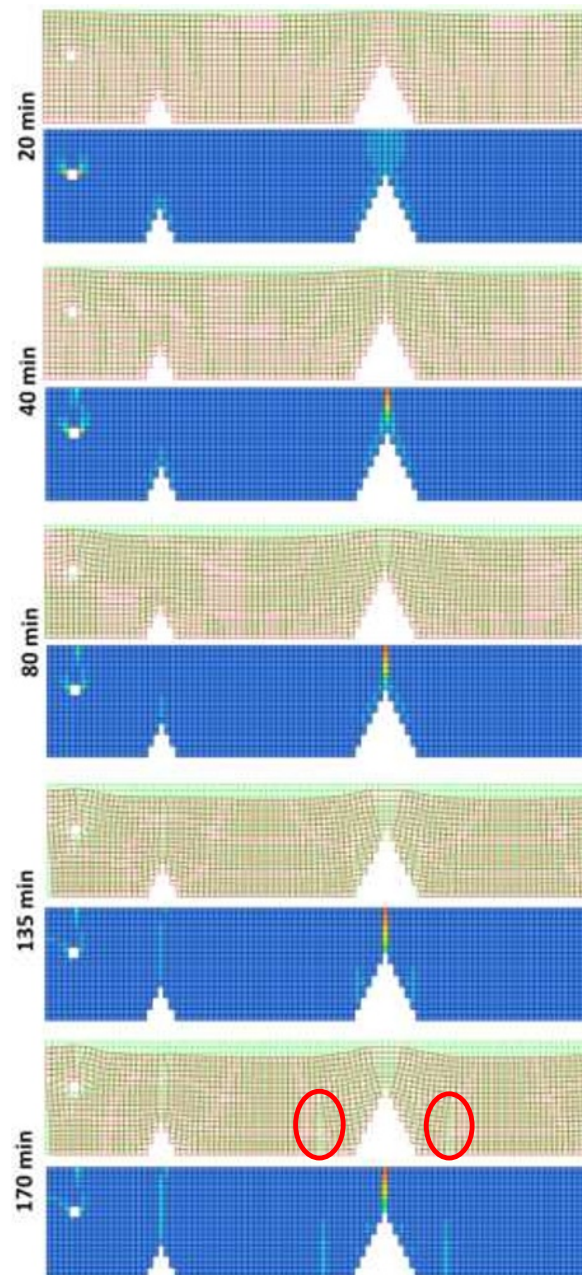


Fig. 8. Modelling results at the extreme climate showing the resultant displacement and maximum principal tensile strain at selected times.

The assumption made that for the finite element model there is no adhesion and/or friction between the concrete and the mould, is the reason the cracks next to the central restraint are present in the analysis and not observed in the experiments. Therefore the cracks from the bottom also occurs next to the centre stress riser. In reality the deformation causing these cracks is smeared out. It is however believed that this lack of friction in the analysis has no effect on the cracks at the top. The incorporation of friction into the model would decrease the severity of these cracks. Especially since these cracks occurred rather late in the analysis long after the central main crack has formed and since the concrete has obtained some strength and therefore also increased friction at this stage. However, it was decided not to add friction to the model, as there is currently no information available regarding

appropriate friction values and since these friction values are also time dependent which would over complicate an already complex time-dependent model.

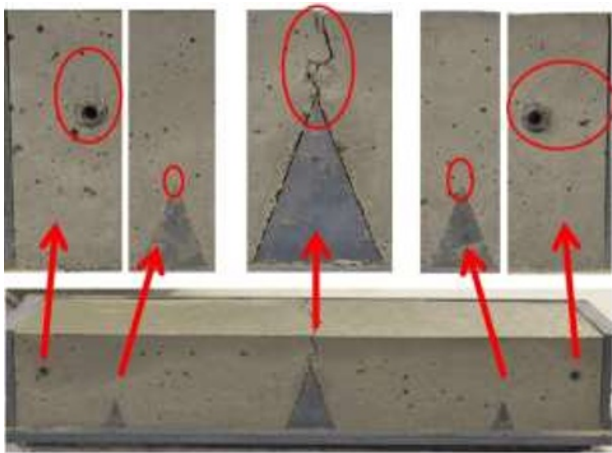


Fig. 9. Images of typical final cracks observed from the side during experiments with the ASTM C1579 [15] based mould at the extreme climate.

As alternative to the incorporation of friction to the model, two additional crack layouts are used for analyses to account for cracks that formed at inappropriate locations such as next to the central restraint. For the first of these analysis, referred to as the singular crack layout analysis, only the column of elements above the central restraint are allowed to crack. For the second analysis, referred to as the selective crack layout analysis, only the elements around the steel bars and the smaller triangular restraints are allowed to crack. Both these crack patterns as well as the first crack pattern where all elements are given cracking behaviour, referred to as the full crack layout, are shown in Fig. 10.

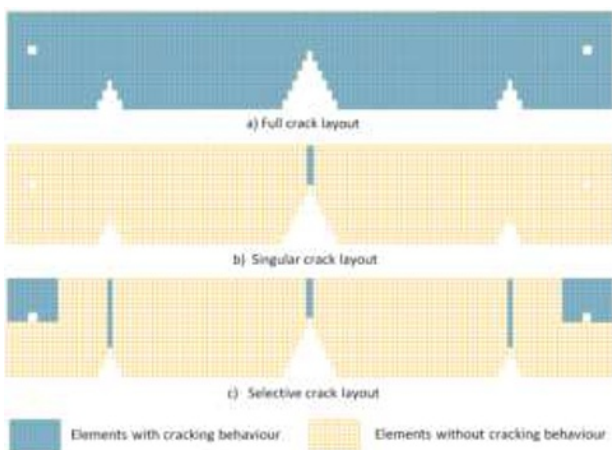


Fig. 10. Finite element mesh layout showing the elements with crack material properties for: a) Full crack layout. b) Singular crack layout. c) Selective crack layout.

Fig. 11 shows the model results of crack width for all three crack layouts as well as the experimental crack widths for each of the samples tested at the extreme climate. The final crack size is arguably the most important evaluation criteria as it gives an indication of the final cracking severity. Fig. 11 shows that the final

crack width obtained during the full crack layout analysis is similar to the cracks observed during experiments, although more towards the lower end or less severe cracks of the experiments. This is because of the severity of cracks that formed at locations other than the main crack above the central restraint. As mentioned several of these cracks are more pronounced in the analysis than the experiments, especially the cracks that formed next to the central restraint during the analysis as indicated with the red circles in Fig. 8.

For the singular crack layout analysis, the crack width results are towards the higher end of the experimental results. This is since all of the crack growth due to shrinkage and settlement is isolated at this single crack location. Furthermore, the results of the selective crack layout analysis give the best representation of the experiments and fit as can be expected between the results of the full and singular crack layout analyses.

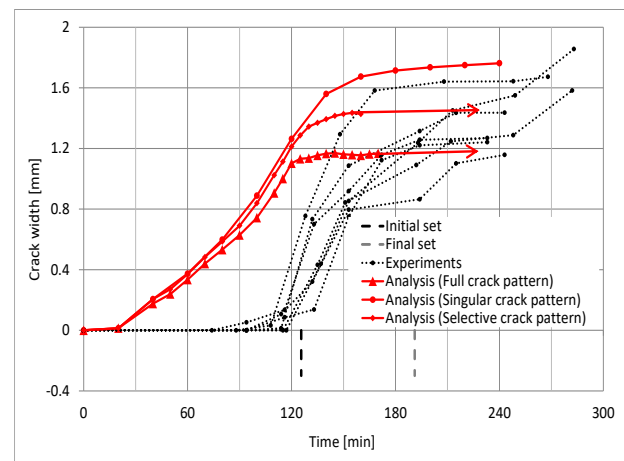


Fig. 11. Crack width results obtained with model for all three crack patterns compared to crack width obtained during experiments at the extreme climate.

From Fig. 11 it can also be seen that the three different crack layout analyses are initially reasonably similar and only start to diverge at around 120 minutes, which is also the time in the analysis where, if allowed, significant crack growth started to occur at locations other than the crack above the central restraint. It should also be mentioned that for the full and selective crack layout analyses more time steps are needed to avoid divergence during the analysis. Furthermore, even with more time steps these analyses started to diverge once the crack growth above the central restraint started to stabilise, partly due to the widening of cracks at other locations as well as the low amount of settlement and shrinkage active at that stage. For these reasons, it was decided to rather use the more stable singular crack layout for the majority of analyses to follow in this paper.

In terms of the time of crack onset and rate of crack growth the analyses and the experiments do not compare as well as for the final crack size. The cracking during analyses occurred much earlier than during experiments, while once formed, the cracks widened at a much higher rate in the experiments than in the analyses. There are two reasons for the earlier and slower rate of cracking in the analyses compared to the experiments.

The first reason is the lower strain capacity of the concrete in the analyses compared to the much higher strain capacity measured during experiments. This is especially noticeable for the first few hours while the concrete is still highly plastic as can be seen in Fig. 12. The figure shows the measured strain capacity during experiments as well as the strain capacity used as input values for the analyses at both 23 and 40°C.

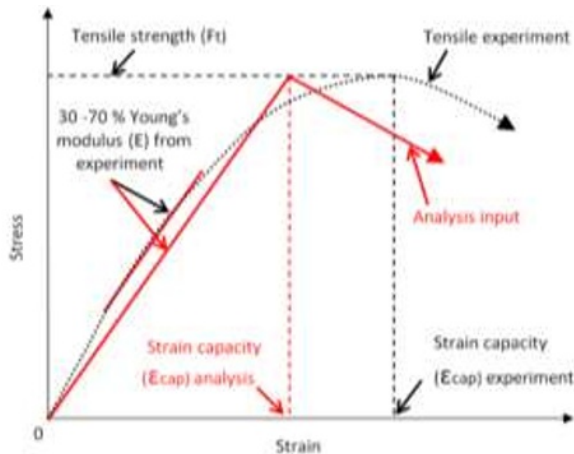


Fig. 12. Illustration of the determination of the strain capacity as used for analyses (indicated in red) as well as the actual strain capacity of the concrete from experiments (indicated in black).

The reason for the smaller strain capacity for the analyses is because of the 30 - 70 % method used to determine the Young's modulus of the fresh concrete during the tensile testing as illustrated in Fig. 12. The figure illustrates the determination of the strain capacity as used for the analysis and linked to the 30 - 70 % method to determine the Young's modulus as well as the actual strain capacity of the concrete from experiments.

The Young's modulus is used together with the results of tensile strength, obtained during tensile testing, as input values for the analyses. The analyses use these input values to calculate the strain capacity by assuming a linear elastic material behaviour in the ascending part of the stress-strain curve. This assumption of linear elastic material behaviour does not account for the significant non-linear strain or strain capacity that especially the still highly fresh concrete exhibits before failure or cracking at maximum tensile strength. This resulted in the analyses predicting earlier cracks than what was observed during experiments.

It should be noted that any traditional method for determining the Young's modulus would even further increase this underestimation of the strain capacity. The more appropriate method to ensure that the correct strain capacity is modelled is to use a bi-linear or even multi-linear approximation of the ascending portion of the stress-strain curve. However, in the current implementation of the model any multi-linear stress-strain curve, especially with regards to the ascending portion, cannot be combined with the method used to model the time-dependency of the material properties. For these reasons the 30 - 70 % method was chosen and used to determine the Young's modulus for the analyses.

The second reason for the earlier and slower rate of cracking in the model compared to the experiments is the difficulty in observing and measuring cracks on the surface of fresh concrete during experiments. The earlier the cracks occur and the smaller the crack, the less visible the crack and the more difficult to measure, especially within the first few hours where the cracks are often still filled with bleed water. Furthermore, as confirmed by Meyer and Combrinck [22], these cracks can even be present beneath the concrete surface and therefore not be visible if viewed from above. This means that the experimental results presented only show the onset of cracking once the cracks were clearly visible with the eye and therefore do not include any possible preceding micro cracking. The analysis can however capture the most insignificant crack. This resulted in the experimental results showing slightly delayed and less severe onset of cracking compared to the analyses. If both these reasons of strain capacity and crack visibility are taken into account, the difference between the time of crack onset and rate of cracking between the analyses and the experiments become much less as illustrated in Fig. 13.

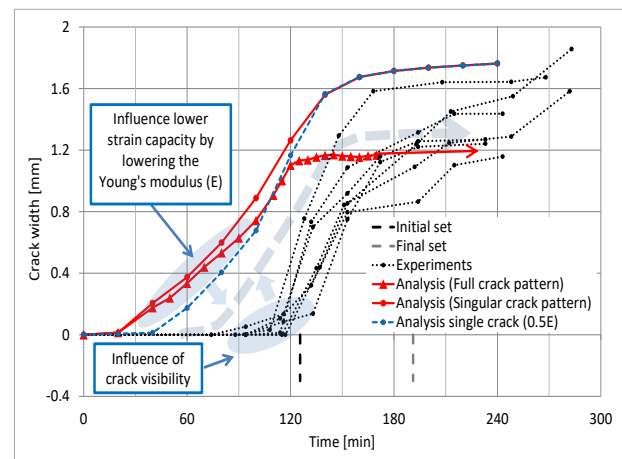


Fig. 13. Influence of strain capacity and crack visibility on the crack width results obtained at the extreme climate.

4.2. Model validation at moderate climate

The results showed that the size and crack onset of the modelled cracks were much smaller and start later with time than for the results at the extreme climate.

The final sizes of the cracks in the analyses were more than twice the sizes of the cracks observed during experiments. The main reason for this significant difference between the experimental and analyses results was the size discrepancy between interior and surface cracks as observed during experiments at the moderate climate. The experimental tests showed that for the moderate climate the interior crack below the concrete surface was notably larger than the measured surface crack, while for the extreme climate the interior and surface cracks were similar.

The reason for this size discrepancy between the surface and interior crack at the moderate climate was the high amount of bleed water on the concrete surface during tests. This crust layer consisted of ultra-fine cement and dust particles that were kept in suspension by the surface

tension of the water. This crust layer often completely or partly obstructed the visibility of the crack at the surface.

4.3. Parameter study

A parameter study was conducted to investigate the influence of variable input values on the results obtained with the model. The input parameters investigated consist of both material properties as well as settlement and shrinkage strains. During each of the analyses conducted for the parameter study, only the applicable parameter (material property, settlement strain or shrinkage strain) was varied while all the other parameters remain unchanged.

For the tensile strength and Young's modulus the variation of input values mainly influenced the time of crack onset and rate of cracking. The larger the tensile strength and the lower the Young's modulus, the later the onset of cracking, but also the greater the rate of cracking once initiated.

The larger the tensile strength and the lower the Young's modulus, the higher the strain capacity of the concrete in the analyses and therefore the later the onset of cracking, which improved the correlation between the experimental and analyses results.

For fracture energy, the variation of input values mainly influenced the rate of cracking and not the time of crack onset. The lower the fracture energy the greater the initial rate of cracking but also the lower the later rate of cracking and vice versa. The results also suggested that a decrease in fracture energy has a more significant influence than an increase in the fracture energy. In fact, an increase in fracture energy has a negligible influence on the results. This indicates that the use of the initial fracture energy instead of the total fracture energy in the model does not significantly influence the results obtained with the model. Finally, the results of the parameter study for all three material properties show that the final size and behaviour of the crack from 240 to 360 minutes were not influenced by variations in material properties.

The input parameters that govern the final size and behaviour of the cracks in the model are the settlement and shrinkage strain. For settlement strain, the variation of input values influenced the time of crack onset, rate of cracking as well as the final crack size. The influence of settlement strain become negligible after approximately 240 minutes. The greater the settlement, the earlier the cracking starts as well as the greater the initial rate of the cracking. More importantly, the greater the settlement, the larger the final crack size at 360 minutes. This shows the important role of plastic settlement cracking in not only inducing cracking, but also aggravating the final severity of the plastic cracking.

For shrinkage strain, the variation of input values influences mainly the rate of the cracking. The time of crack onset was not influenced by the variation of the shrinkage strain. The greater the shrinkage the greater the rate of cracking.

5. Conclusions

This paper discussed the approaches to the modelling of cracking in plastic cracking as well as the results achieved with a finite element model of the cracking of fresh

concrete. The following significant conclusions can be drawn:

- The main challenges with the finite element modelling of fresh concrete are: the testing of the fresh concrete to determine the tensile material properties, the time dependency for material properties as well as volume change, the anisotropic nature of volume change in terms of direction, and the appropriate constitutive law needed to govern the behaviour of the fresh concrete under loading.
- The finite element model presented in this paper uses a total strain smeared cracking approach to model the cracking and accounts for both the time dependency of material properties and the anisotropic volume change of fresh concrete.
- The model gives an adequate representation of the cracking behaviour of fresh concrete for extreme climates with high evaporation rates but not for more normal to moderate climates. The reasons for the poor correlation with experimental results at moderate climates are the size discrepancy between the interior and surface cracks during experiments as well as the relaxation of stresses in fresh concrete that are not accounted for in the model.
- The model also predicts an earlier onset of cracking compared to the experiments with the reasons believed to be the lower strain capacity used in the analyses as well as the difficulty in observing and measuring cracks on fresh concrete during experiments.
- The parameter study showed that both the settlement and shrinkage strains significantly influence and therefore govern the size of the final crack, while the material properties only influence the time of crack onset and rate of crack widening.

References

1. R.E. Weyers, J.C. Conway, P.D. Cady, *Cem. and Conc. Res.* 12:475-484 (1982).
2. H.G. Kwak, S. Ha, W.J. Weiss, *Jour. of Mat. in Civ. Eng.*, 22(10):951-966 (2010).
3. R. Combrinck, L. Steyl, W.P. Boshoff, *Cons. and Build. Mat.*, (175) 621-628 (2018).
4. F.H. Wittmann, *Cem. and Conc. Res.*, 6(1):49-56 (1976).
5. V. Slowik, M. Schmidt, R. Fritzsche, *Cement & Concrete Composites*, 30:557-565 (2008).
6. P.J. Uno, *ACI Mat. Jour.*, 95(4):365-375 (1998).
7. ACI 308R, American Concrete Institute (2001).
8. J.S. Dolado, K. Van Breugel, *Cem. and Conc. Res.*, 41:711-726 (2011).
9. V. Slowik, M. Schmidt, T. Hubner, B. Villmann, *Cem. & Conc. Comp.*, 31:461-469 (2009).
10. H.G. Kwak, S.J. Kim, *Build. & Env.* 41(10) (2006).
11. V. T. Dao, P. F. Dux, P. H. Morris, *ACI Materials Journal*, 106(6):483-492 (2009).

12. R. Combrinck, W.P. Boshoff, 2019, *Cement and Concrete Composites* 97, (300-311) (2019).
13. ASTM C469, ASTM International (2014).
14. EN 12390-13, UK: British Standards Institute (2013).
15. ASTM C 1579, ASTM International (2006).
16. R. De Borst, *Eng. Frac. Mech.*, 69:95-112 (2002).
17. R. Combrinck, Stellenbosch: The University of Stellenbosch. (PhD thesis), (2016).
18. Diana Software Package Version 9.6, *User's manual* (2010).
19. Z.P. Bazant, B.H. Oh, *Materials and Structures*, 16(93):155-177 (1983).
20. Y.-J. Li, T. Zimmerman, *Comp. & Struc.*, 69: 487-497 (1998).
21. R. Combrinck, W.P. Boshoff, *Mag. of Con. Res.*, 65(8) (2013).
22. D.M. Meyer, R. Combrinck, *Const. & Build. Mat.* 317 (2022).